Journal of Civil Engineering (IEB), 41 (2) (2013) 179-199

Journal of Civil Engineering IEB

Effect of soil-structure interaction on seismic response of a seismically isolated highway bridge pier

A. K. M. T. Alam[1] and M. A. R. Bhuiyan[2]

[1] *Department of Disaster and Environmental Engineering*
[2]*Department of Civil Engineering*
Chittagong University of Engineering and Technology, Chittagong 4349, Bangladesh

Received 01 November 2013

Abstract
This study is dedicated towards conducting seismic performance evaluation of a seismically isolated highway bridge pier incorporating the soil-interaction, subjected to low to medium far field earthquake ground accelerations. Laminated rubber bearings (LRB), manufactured using high damping rubber material, are used in the seismic isolation of the bridge pier. In seismic performance evaluation of the pier, nonlinear dynamic analysis using a standard direct time integration approach has been carried out by incorporating the nonlinear mechanical behaviour of the isolation bearing, pier and footing-soil. A visco-elasto-plastic rheology model of LRB, a bilinear force-displacement relationship for pier and an equivalent linear model for footing-soil interaction are employed in the analysis for realizing their mechanical behaviour under seismic excitations. The equivalent linear model used for understanding the soil-structure interaction between footing and its surrounding soil comprises linear translational spring and dashpot components. The seismic responses of the bridge pier considered in the performance evaluation are footing displacement, pier displacement, bearing displacement and deck displacement. The analyses results have revealed that soil-structure interaction effects may be neglected in the seismic analysis of seismic-isolated bridges constructed on stiff/very hard soil; however, the soil-structure interaction effects need to be carefully considered for bridges constructed in soft soil conditions.

Keywords: Visco-elasto-plastic rheology model; nonlinear dynamic analysis; foundation stiffness; laminated rubber bearing

1. Introduction

Seismic isolation has been considered to be an efficient technology for providing mitigation to seismic damages for highway bridges, and has proven to be reliable and cost effective.

More than 200 bridges have been designed or retrofitted in Japan and in the United States using seismic isolation in the last 20 years, and more than a thousand of bridges around the world now use this cost- effective technique for seismic protection, for example, the 29-span continuous O-Hito viaduct in Japan and the seven-span continuous steel girder Lake Saltonstall bridge in USA, etc.. In order to improve the seismic performance for both new and retrofitting applications, different forms of seismic isolation devices have widely been employed for the last few decades (Naeim and Kelly, 1996; Kelly, 1997). Seismic isolation is meant to shift the natural period of a bridge structure in such a way that the dominant frequency of the earthquake ground acceleration can safely be avoided to safeguard it against the seismic damage. In addition, the inherently occupied damping property and energy dissipation mechanism prevents the bridge system from over displacement (Kelly, 1997; Skinner et al., 1993). Field evidence on the seismic response of isolated bridges during recent earthquakes (Chaudhary et al., 2001), experimental research (Hwang et al., 2002; Kikuchi and Aiken, 1997) as well as analytical studies (Ghobarah and Ali, 1988; Ozbulut and Hurlebaus, 2011a, b; Zhang and Huo, 2009; Wilde et al., 2000) have indicated that isolation devices can effectively improve the structural seismic resistance and consequently reduce the cost for repair and rehabilitation after earthquakes.

It is well recognized that soil-structure interaction (SSI) could play a significant role on structural response of highway bridges. The safe and economic seismic designs of bridge structures depend directly on the understanding level of seismic excitation and the influence of supporting soil on the structural dynamic response. Long span bridges are susceptible to relatively more severe soil structure interaction effect during earthquakes as compared to buildings due to their spatial extent, varying soil condition at different supports and possible incoherence in the seismic input. The seismic response of highway bridges is usually evaluated assuming the free-field motion at their bases. This hypothesis is in principle acceptable when the soil is very stiff and soil-structure interaction (SSI) effects are negligible. The effects of (SSI) and the contribution of the higher modes of vibration are commonly ignored in the earthquake resistant design of seismically isolated bridges. These simplifications are done assuming that the flexibility of the isolation system and the isolated modes of vibration dominate the seismic behaviour of the bridge. Only limited research has been conducted to study the effect of SSI on the performance of seismic-isolated bridges (Chaudhary et al. 2001, Vlassis and Spyrakos (2001), and buildings, Todorovska 1996, Dasgupta et al., 1999). The inclusion of SSI phenomena in the seismic analysis and design of structures is addressed in seismic code provisions, including the recent FEMA 450 document (FEMA450 2003). Several studies have been made to assess the effect of SSI phenomena on the seismic response of base-isolated bridges. Chaudhary et al. (2001) have identified the structural and geotechnical parameters of four base-isolated bridges using available theoretical models and data from recent earthquakes. The main conclusions of their study are that SSI effects depend primarily on horizontal pier stiffness in relation to the soil horizontal stiffness, and that the important reduction in the soil shear modulus for moderate earthquakes should be definitely incorporated into SSI analyses. Tongaonkar and Jangid (2003) presented the SSI effects on a three-span bridge with LRBs, assuming frequency independent expressions for the soil stiffness and damping parameters. Their numerical study revealed an increase in the seismic displacements when SSI is included, a fact that should be taken into account for the design of bridges. Therefore, further research is required in this area to guide the design engineers to have built more accurate structural models of seismic-isolated bridges that may lead to more improved prediction of their seismic response.

The objective of this study is to conduct seismic performance evaluation of a seismically isolated highway bridge pier incorporating the soil-interaction, subjected to low to medium far field earthquake ground accelerations. Laminated rubber bearings (LRB),

manufactured using high damping rubber material, are used in the seismic isolation of the bridge pier. In seismic performance evaluation of the pier, nonlinear dynamic analysis using a standard direct time integration approach has been carried out by incorporating the nonlinear mechanical behaviour of the isolation bearing, pier and footing-soil. A visco-elasto-plastic rheology model of LRB, a bilinear force-displacement relationship for pier and an equivalent linear model for footing-soil interaction are employed in the analysis for realizing their mechanical behaviour under seismic excitations. The equivalent linear model used for understanding the soil-structure interaction between footing and its surrounding soil comprises linear translational spring and dashpot components. The seismic responses of the bridge pier considered in the performance evaluation are footing displacement, pier displacement, bearing displacement and deck displacement. The analyses results have revealed that soil-structure interaction effects may be neglected in the seismic analysis of seismic-isolated bridges constructed on stiff/very hard soil. However, the soil-structure interaction effects need to be considered for bridges constructed in soft soil conditions.

Table 1
Geometries and material properties of the bridge

Properties	Specifications
Cross-section area of the pier body (mm^2)	19643000
Height of the pier (mm)	7000
Young's modulus of elasticity of concrete (N/mm^2)	25000
Young's modulus of elasticity of steel (N/mm^2)	200000

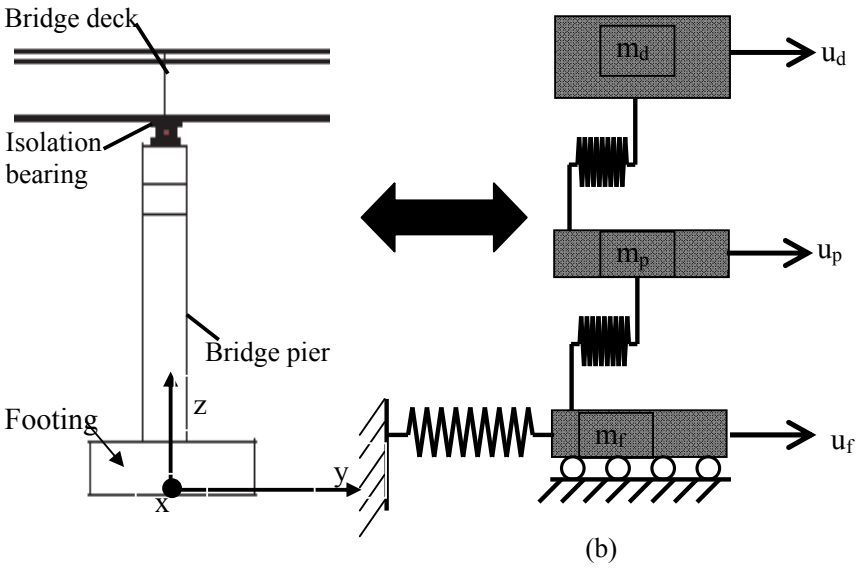

Fig. 1. Modelling of the bridge pier

2. Modeling of the Bridge

2.1 Physical model

A typical interior pier of a multi-span continuous highway bridge, isolated laminated rubber bearing (LRB), is used in this study shown in Fig. 1 (a). The bridge consists of continuous reinforced concrete (RC) deck with prestressed concrete (PC) girders isolated by LRB, installed below PC girders and supported on RC piers. The superstructure consists of 200 mm RC slab covered by 80 mm of asphalt layer. The mass of a single span bridge deck is $1200x10^3$ kg and that of a pier is $250x10^3$ kg. The substructure consists of RC pier and RC footing supported on shallow spread footing. The effective mass of the footing with surrounding soil is approximated as $180x10^3$ kg. The dimensions and material properties of the bridge deck and pier with footings are given in Table 1. The geometry and material properties of LRB are presented in Table 2.

Table 2
Geometries and materials properties of the isolation bearings

Dimension	values
Cross-section of the bearing (mm^2)	100000
Thickness of rubber layers (mm)	175
Number of rubber layers	6
Thickness of steel layer (mm)	3.0
Nominal shear Modulus of rubber (MPa)	1.2

2.2 Analytical model

2.2.1 Equations of motion of the bridge pier

The analytical model of the bridge system is shown in Fig. 1(b). The bridge model is simplified into a three-degree of freedom (3-DOF) system. This simplification holds true only when the bridge superstructure is assumed to be rigid in its own plane which shows no significant structural effects on the seismic performance of the bridge system when subjected to earthquake ground motion (Ghobarah, 1988; Ghobarah and Ali, 1988). The mass proportional damping of the bridge pier is considered in the analysis.

Dynamic soil–structure interaction problems can be treated in different ways. Exact or rigorous analysis could be obtained only under certain specific conditions. The most direct approach to solve the problem is to include a layer of the soil along with the structure and use the finite element approach to model the entire system. Equations that govern the dynamic responses of the 3-DOF system can be derived by considering the equilibrium of all forces acting on it using the d'Alermbert's principle. In this case, the internal forces are the inertia forces, the damping forces, and the restoring forces, while the external forces are the earthquake induced forces. Equations of motion are given as

$$m_d\ddot{u}_d(t)+F_{is}(u_p,\dot{u}_p,u_d,\dot{u}_d,t)=-m_d\ddot{u}_g(t), \tag{1a}$$

$$m_p\ddot{u}_p(t)+F_p(u_p,t)-F_{is}(u_p,\dot{u}_p,u_d,\dot{u}_d,t)=-m_p\ddot{u}_g(t), \tag{1b}$$

$$m_f \ddot{u}_f(t) - F_p(u_p, t) + F_f(u_f, \dot{u}_f, t) = -m_f \ddot{u}_g(t) \tag{1c}$$

where m_p , m_d , m_f , u_p , u_d , u_f are the masses and displacements of pier, deck and effective footing respectively. $\ddot{u}_p$, $\ddot{u}_d$, $\ddot{u}_f$ are the accelerations of pier, deck and foundation, respectively. $\ddot{u}_g$ is the ground acceleration. $F_p(u_p, t)$ is the internal restoring force of the pier to be evaluated by bilinear model (Ghobara and Ali, 1988). The nonlinear force-displacement relation (i.e. the bilinear model) is employed to take into account for the nonlinear force-displacement behaviour of the bridge pier. $F_{is}(u_p, u_d, \dot{u}_p, \dot{u}_d, t)$ is the restoring force of the isolation bearings. For LRB, it is computed using Eq.(2) and becomes $F_{is}(u_p, u_d, \dot{u}_p, \dot{u}_d, t)$. $F_p(u_p, \dot{u}_p, t)$ is the restoring force to be evaluated by using the equivalent linear model. The equivalent linear model of the foundation is represented by a linear spring and a linear dashpot element. The rotational stiffness of the soil-foundation system is excluded from the idealized model for the purpose of simplicity. The unconditionally stable Runge Kutta 4th order method is used in the direct time integration of the equations of motion (Eqs. (1)).

2.2.2 Modelling of Laminate Rubber Bearing (LRB)

The experimental investigations conducted by several authors (Bhuiyan et al., 2009; Hwang et al., 2002; Imai et al., 2010; Miehe and Keck, 2000) have revealed four different fundamental properties, which together characterize the typical overall response of laminated rubber bearings: (i) a dominating elastic ground stress response, which is characterized by large elastic strains (ii) a finite elasto-plastic response associated with relaxed equilibrium states (iii) a finite strain-rate dependent viscosity induced overstress, which is portrayed by relaxation tests, and finally (iv) a damage response within the first cycles, which induces considerable stress softening in the subsequent cycles. Considering the first three properties, a strain-rate dependent constitutive model for the LRB is developed by Bhuiyan(2009), which is verified for sinusoidal excitations and subsequently implemented in professional structural engineering software (Resp-T, 2006) for conducting seismic performance analysis of multi-span continuous highway bridge (Bhuiyan, 2009; Razzaq et al., 2010).

Eqs. 2(a) to 2(d) provide the explicit expressions for the average shear stress τ and strain γ of the bearings. A rigorous experimental investigation has been carried by Bhuiyan (2009) to identify the parameters of the model. For more discussion, the readers are requested to refer to the earlier efforts by Bhuiyan (2009), Imai et al. (2010) and Bhuiyan and Okui (2012)

$$\tau = \tau_{ep}(\gamma_a) + \tau_{ee}(\gamma) + \tau_{oe}(\gamma_c) \tag{2a}$$

$$\tau_{ep} = C_1 \gamma_a \text{ with} \begin{cases} \dot{\gamma}_s \neq 0 & \text{for } |\tau_{ep}| = \tau_{cr} \\ \dot{\gamma}_s = 0 & \text{for } |\tau_{ep}| < \tau_{cr} \end{cases} \quad \text{and } \tau_{cr} = S_1 + S_2 |\gamma_{\max}| \tag{2b}$$

$$\tau_{ee} = C_2 \gamma + C_3 |\gamma|^m \operatorname{sgn}(\gamma) \tag{2c}$$

$$\tau_{oe} = C_4 \gamma_c \text{ with } \tau_{oe} = A \left| \frac{\dot{\gamma}_d}{\dot{\gamma}_o} \right|^n \operatorname{sgn}(\dot{\gamma}_d) \tag{2d}$$

and $A = \frac{1}{2}\left(A_1 \exp\left(q|\gamma|\right) + A_u\right) + \frac{1}{2}\left(A_1 \exp\left(q|\gamma|\right) - A_u\right)\tanh\left(\xi\tau_{oe}\gamma_d\right)$

where C_i (i = 1 to 4), S_i (i = 1 to 2), τ_{cr}, m, A_l, A_u, q n and ξ are the model parameters determined from a number of experiments (Bhuiyan, 2009) and are listed in Table 3.

Table 3
Parameters for LRB (Bhuiyan, 2009)

Parameters	Values
C_1 (MPa)	2.54
C_2 (MPa)	0.48
C_3 (MPa)	0.0086
C_4 (MPa)	3.25
m	5.18
A_l (MPa)	0.4
A_u (MPa	0.20
q	0.34
n	0.22
S_1 (MPa)	0.077
S_2 (MPa)	0.097
ξ	1.22

2.2.3 Modelling of bridge pier

Four types of hysteresis loops of reinforced concrete structures are usually used in the nonlinear dynamic analysis of a bridge structure: elasto-plastic model, bilinear model, Clough model, and tri-linear Takeda model. The force-displacement curve as represented by elasto-plastic model is far away from the experimental observations. Upon yielding of the section, no incremental stiffness is assumed; at load reversal stage, no stiffness degradation is considered. Considering the poor agreement between the hysteretic behaviour predicted by the elasto-plastic model and the experimental observations of typical reinforced concrete structural elements, the use of this model for predicting the hysteretic behaviour of reinforced concrete structures is not justified. However, some uses of this model are apparent in the time-history analysis of reinforced concrete frames due to its simplicity of modelling (Saiidi, 1982). Bilinear model is almost similar to the elasto-plastic model except for the fact that the strain hardening effect beyond yielding of the steel material is considered in this model. Although it seems to be more realistic than the elasto-plastic model, the bilinear model cannot consider the stiffness degradation during unloading and load reversals. By the similar reasons as stated in the case of the elasto-plastic model, the bilinear model is also not well justified for using in the response history analysis of the reinforced concrete structures (Saiidi, 1982). Clough's degrading stiffness model is somewhat more realistic than the two preceding models. This model has included stiffness degradation phenomenon during the load reversals. However, the stiffness degradation in the unloading is not incorporated in the model. As a result, this model is deemed to be less accurate than currently adopted tri-linear model since the former one has resulted overestimation of the stiffness and energy dissipation of reinforced concrete structural members subjected to relatively small amplitude displacement or load that falls between cracking and yield (Ghobarah and Ali, 1988; Saiidi, 1982). The Takeda model is one of the most realistic hysteretic model for reinforced concrete structures. This model was developed based on experimental observations conducted on many reinforced

concrete joints and specimens under static cyclic loading (Takeda, 1970). This model was shown to be successful in predicting the static and dynamic behaviour of reinforced concrete joints and elements (Takeda et al., 1970). This model is, however, computationally very expensive and that's why the bilinear and the Clough's degradation models are widely used in the seismic response analysis of highway bridge for simplicity in use. The current study uses the bilinear model as shown Fig. 2 to simply idealize the nonlinear force-displacement behaviour of the bridge pier by incorporating two stiffness components (k_o and k_p) and a characteristic yield strength (F_y) parameter. The former stiffness component is the elastic stiffness and the latter one is the post-yield stiffness. The three parameters of the model are evaluated from a push-over analysis of the bridge pier, which are presented in Table 4.

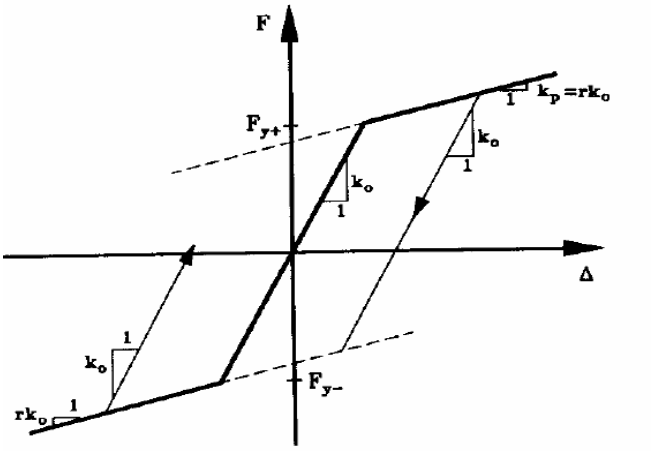

Fig. 2. Bilinear model of the bridge pier

Table 4
Parameters of the bilinear model

Parameters	Values
k_o (kN/m)	67000
k_p (kN/m)	6700
F_y (kN)	4500

2.2.4 Modelling of Soil-Footing interaction

For the seismic analysis of overground and underground structures, consideration of the soil–structure interaction becomes extremely important when the soil or the foundation medium is not very firm. During earthquake excitation, the structure interacts with the surrounding soil imposing soil deformations. These deformations, in turn, cause the motion of the supports or the interface region of the soil and the structure to be different to that of the free field ground motion. These interactions substantially change the response of the structure. For very stiff soil, this change is extremely small and can be neglected. Therefore, consideration of base fixity remains a valid assumption for overground structures constructed on firm soil. The effect of a dynamic soil–structure interaction depends on the stiffness and mass properties of the structure, the stiffness of the soil, and the damping characteristics of both soil and structure (Datta, 2010). The dynamic soil–structure interaction consists of two interactions, namely, kinematic interaction and inertial interaction. The kinematic interaction is the result of the stiffness of the structure, while the inertial interaction is the result of the mass of the structure (Datta, 2010).

It is widely accepted that the effects of the ground conditions should be considered in the seismic performance analysis of highway bridge, especially when the bridge utilizes the seismic isolation devices (JRA, 2002). Generally, three types of ground conditions are considered: Ground Type-I, Type-II and Type-III. These classifications are made in accordance with the ground characteristic value T_G (Table 5). The value of T_G can be estimated using Eqn. (3).

$$T_G = 4\sum_{i=1}^{n} \frac{H_i}{V_{si}} \tag{3}$$

where T_G is the characteristic value of soil (s), H_i is the thickness of the i^{th} soil layer (m) , n is the number of soil layers and V_{si} is the average shear elastic velocity of the i^{th} soil layer which can be evaluated using the standard penetration values (N), if there is no measured value available. This value is usually measured by elastic wave propagation or PS logging (JRA, 2002). In different highway bridge design specifications, such as JRA (2002), it is recommended to avoid the needless complicacy in estimating the elastic shear velocity of soil layer V_{si} , rather the following equations are recommended to use for this purpose:

$$V_{si}(m/s) = 100N_i^{1/3} \quad 1 \le N_i \le 50 \quad \text{for cohesive soil layer} \tag{4}$$
$$V_{si}(m/s) = 80N_i^{1/3} \quad 1 \le N_i \le 50 \quad \text{for sandy soil layer}$$

Table 5
Ground types in seismic design (JRA, 2002)

Ground Type	Characteristic Value of Ground, T_G (s)
Type-I	$T_G < 0.2$
Type-II	$0.2 \le T_G < 0.6$
Type-III	$0.6 \le T_G$

Generally, Type-I ground includes good alluvial ground and rock, Type-III ground includes soft ground of alluvial ground and Type-II ground denotes diluvial and alluvial ground not belonging to Type-I and Type-III.

Foundations of bridge piers are the structural elements at or below ground level that support the pier and provide vertical, lateral and rotational resistance to gravity loads and seismic forces. The way in which this resistance is developed depends on (1) the type and geometry of the foundation, (2) the characteristics of surrounding soil, and (3) the interaction between soil and structure (Preistley et al., 1996). In the current study, the spread footing has been used in the analysis, which is typically considered to be rigid body that allows support conditions to be modelled at a single point with boundary springs at the bottom of the bridge pier model at the end of effective length extension link into the footing. For a two dimensional bridge pier, only a vertical, a translational and a rotational boundary springs need to be defined whereas in a three dimensional model, six springs, one for each possible degree of freedom at the pier base, are considered (Preistley et al., 1996). In the spread footing the soil resistance is provided in the vertical directions by direct bearing pressure, in the horizontal direction by passive soil pressure in front of the footing and friction along the footing base, and in

rotational direction by the soil overburden on top of the footing and gravity-load effects. The rotation is usually considered only when uplift and rocking of the entire footing can occur. Considering the coordinate axes as shown in Fig. 1 (a) the spring constants of the ground are expressed (JRA, 1996) as:

$$\begin{Bmatrix} F_y \\ M_x \\ F_z \end{Bmatrix} = \begin{bmatrix} K_y & K_{y\theta x} & 0 \\ K_{y\theta x} & K_{\theta x} & 0 \\ 0 & 0 & K_z \end{bmatrix} \begin{Bmatrix} \delta_y \\ \theta_x \\ \delta_z \end{Bmatrix} \tag{5}$$

where, F_y, F_z are the forces acting on the foundation in the y-translational and vertical (z axis) directions (tf); M_x is moment around the x-axis acting on the foundation (tf.m) δ_y, δ_z are the displacements of the foundation in the y-translational and vertical direction (z axis) (m); θ_x is rotation angle of the foundation around the x-axis (rad); K_y, K_z are the spring constants of the ground in the translational and vertical directions (tf/m); $K_{\theta x}$ is rotational spring constant of the foundation around the x-axis (tf.m/rad); $K_{y\theta_x}$ is coupling spring constant of the foundation of the displacement in the y-direction and rotation around the x-axis (tf.m/m)

Equation (6) shows the spring constants of the ground:

$$\left.\begin{aligned} K_y &= k_{SB} A_B \\ K_z &= k_v A_B \\ K_{\theta x} &= k_v I_B \\ K_{y\theta x} &= 0 \end{aligned}\right\} \tag{6}$$

where, k_{SB} is the subgrade shear reaction coefficient at the bottom of the footing (tf/m^3); k_v is the subgrade vertical reaction coefficient at the bottom of the foundation (tf/m^3); A_B is the area of the footing at the bottom(m^2); I_B is the area moment of inertia of the footing (m^4)

The vertical subgrade reaction coefficient k_v and the horizontal subgrade reaction coefficient k_{SB} are obtained from the following Eqn. (7):

$$\left.\begin{aligned} k_v &= k_{vo}\left(\frac{B_v}{30}\right)^{-3/4} \\ k_{SB} &= \lambda k_v \\ B_v &= \sqrt{A_v} \end{aligned}\right\} \quad \text{with} \quad k_{vo} = \frac{1}{30} E_D \text{ and } E_D = 2(1+\nu_D)\frac{\gamma_s}{10g} V_{si}^2 \tag{7}$$

where, k_{vo} is the standard value of vertical subgrade reaction coefficient at the bottom of the footing (kgf/cm^3); k_{SB} is the horizontal subgrade reaction coefficient at the bottom of the footing (kgf/cm^3); A_v is the area of the footing at the bottom(cm^2) ; B_v is the equivalent

surcharge width of the footing (cm); λ is the ratio of horizontal subgrade reaction coefficient to the vertical subgrade reaction coefficient; E_D is the dynamic deformation coefficient of soil (kgf/cm^2); ν_D is the Poisson's ratio of soil ; γ_s is the unit weight of soil (tf/m^3); V_{si} is the average shear elastic velocity of the i^{th} soil layer (m/s) g is the acceleration due to gravity (9.81 m/s^2)

In the current study, for simplicity, only two spring constants for the ground, one in translational direction and one in vertical direction, are considered in the analysis to simulate the soil-structure interaction between footing and the surrounding soils. In the vertical direction the footing may be considered to be rigidly connected with the ground and hence only the horizontal spring constant K_y has been evaluated using the equations stated above. Based on the average elastic shear velocity of the soil layer underneath the footing four values of K_y are considered in the analysis as shown in Table 6. The interaction between footing and surrounding soils has been modelled using a linear spring (i.e., representing translational resistance in terms of spring constant, K_y) and a dashpot (i.e. representing the damping property of surrounding soil in terms of damping ratio). The equivalent viscous damping ratio for surrounding soil of the footing as sued in the analysis is 0.2 in estimating the mass proportional damping of the foundation (JRA, 2002 and 1996).

Table 6
Foundation spring constants K_y

Soil Type	K_y (tf/m)
Very Hard	2600000
Hard	26000
Medium	2600
Soft	260

3. Seismic ground accelerations

Most of the seismic design guidelines are developed based on the characteristics of far-field ground motions. One of the characteristic features is the epicentral distance from building site to the rupturing fault to separate the near field from the far field ground accelerations. According to Caltrans (2004) if the structure under consideration is within 10 miles (approximately 15 km) of a fault can be classified as near-fault. Ground motions outside this range are classified as far-field motions. The current study considers an earthquake ground motion record (EQ-1) (Kanto Earthquake 1923) having PGA of 0.35g, a far-field earthquake ground motion record entitled in JRA (2002). This earthquake ground motion has been considered as a moderate earthquake ground motion (known the Level-2, Type-I earthquake) in the design of Japanese highway bridges (JRA 2002). In consideration of the fault-lines distribution in Bangladesh this ground motion record has been scaled down to 0.25g to approximately simulate a low to moderate earthquake ground record (EQ-2). It is noted that the frequency content, duration of the earthquake ground motion, ground condition and characteristics of faults have significant effect seismic responses. The characteristics of the earthquake ground motion records (EQ-1 and EQ-2) are presented in Figs. 3 (a) and (b). Fig. 3(a) shows ground motion histories and Fig.2 (b) presents the acceleration response spectra with 5 percent damping ratio of the ground motions. From Fig. 3(b), it is seen that the dominant periods of the earthquake ground motion records vary from 0.2 sec to 1.5 sec which cover the wide range of natural periods of seismically isolated highway bridges.

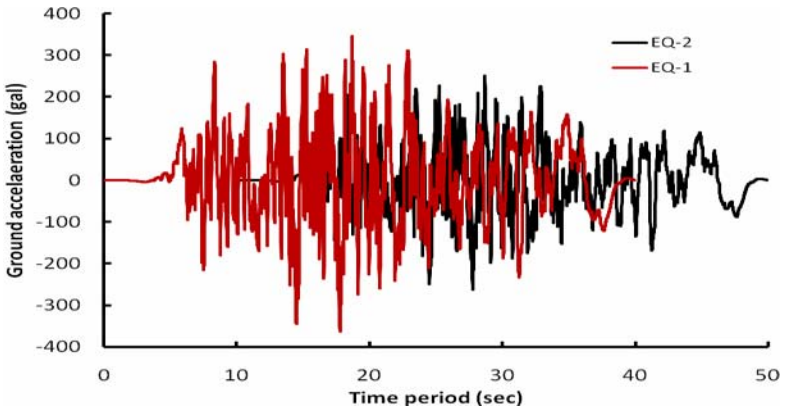

(a)

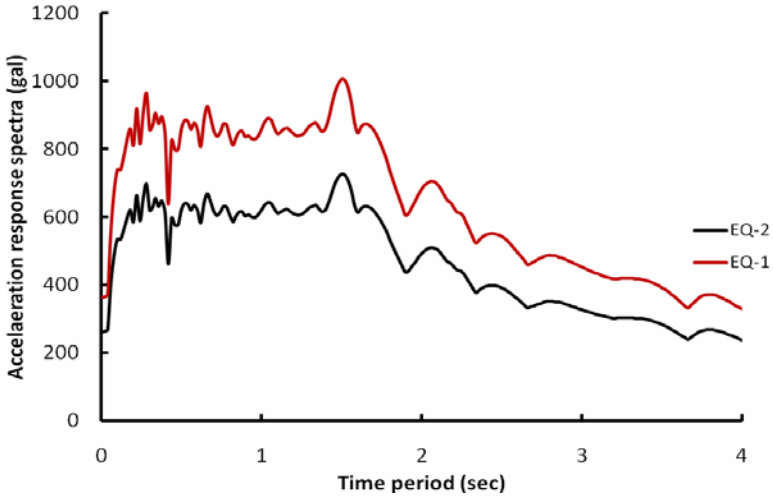

(b)

Fig.3. (a) acceleration-time histories and (b) acceleration response spectra of earthquake ground motion records; for clarity, the ground motion records are separated by 10 sec from each other (a).

4. Numerical results and discussion

Seismic responses of the bridge pier, modelled by a 3-DOF system (Fig. 1), are evaluated for two earthquake ground motion records (EQ-1 and EQ-2) (Fig.3). The peak ground acceleration (PGA) values of the two earthquakes are, 0.35g and 0.25g, respectively, representing far-field earthquake ground motion. The characteristics of the two earthquakes are reasonably the same with reduced spectral ordinates (Fig. 3b). In the 3-DOF system, the seismic isolation bearing has been characterised by a nonlinear visco-elasto-plastic rheology model (Bhuiyan 2009, Bhuiyan et al., 2009 and Bhuiyan and Okui, 2012, etc.), the bridge pier is described by a standard bilinear model and the footing-soil interaction has been characterised by an equivalent linear model, as discussed in Section 2. Seismic responses are evaluated by conducting nonlinear dynamic analysis based on the direct time integration approach using the 4^{th} order Runge-Kutta method. An eigen-value analysis has been carried out to grasp the fundamental dynamic properties of the bridge. The equivalent fundamental natural period of idealized 3-DOF system is evaluated, using Eq. (8), as 1.7 sec.

$$T_e = 2\pi\sqrt{m_p\left(\frac{1}{k_f}+\frac{1}{k_p}\right)+m_f\left(\frac{1}{k_f}+\frac{1}{k_p}+\frac{1}{k_{is}}\right)} \quad (8)$$

where k_f, k_p and k_{is} are equivalent linear stiffness for soil-footing, pier and isolation bearing, respectively.

In comparative assessment of seismic responses of the system, a few standard response parameters obtained for each earthquake are addressed in the subsequent subsections: pier displacement, shear stress and strain of the bearing (LRB), deck displacement of the bridge, and foundation movement. Each response parameter of the bridge pier is computed for the four types of grounds (e.g. soft, medium, hard and very hard) and is compared with that considering a fully restrained ground condition. The simulation results are presented in Figs. 4 to 10. In order to identify the damage states of the bridge components, the definitions of damage states and their corresponding damage criteria available in the literature are given in Table 7.

Table 7
Damage/limit states of bridge components
(Bhuiyan et al., 2012)

Physical phenomenon	Damage State	Displacement ductility μ_d	Shear strain γ (%)
Cracking	Slight (DS=1)	μ_d >1.0	γ >100
Moderate cracking and spalling	Moderate (DS=2)	μ_d >1.2	γ >150
Degradation without collapse	Extensive (DS=3)	μ_d >1.76	γ >200
Failure leading to collapse	Collapse (DS=4)	μ_d >4.76	γ >250

4.1 Pier displacement

The two factors affecting the pier displacement are energy dissipation by the bearings and the forces developed in the bearings. The pier displacement decreases with increase in energy dissipation but increases with increase in the bearing forces. Figs. 4(a) and (b) present the time histories of the pier displacement for the two earthquakes showing a significant difference in responses due to ground conditions in each earthquake. The peak displacements of the pier are presented in Figs. 6(a) and (b) illustrating that the bridge pier produces large displacement in soft soil condition causing, according to Table 7, moderate and slight damage states, respectively, for earthquakes EQ-1 and EQ-2. In the moderate damage states, the bridge pier is expected to have occurred a moderate cracking with spalling of concrete. However, in hard and very hard soil conditions, the bridge pier does not experiences any damage, i.e. the pier displacement is seen to be within the yield displacement, for both earthquakes (EQ-1 and EQ-2). In the medium ground condition, the bridge pier experiences a slight damage state in EQ-1, whereas, no such damage occurs in EQ-2. The pier displacements as obtained for the two earthquakes in a fully restrained ground condition are also superimposed in Figs. 6(a) and (b) as reference values. The pier displacement as obtained

assuming a fully restrained condition at the base of the bridge pier is also superimposed in Figs. 6 (a) and (b).

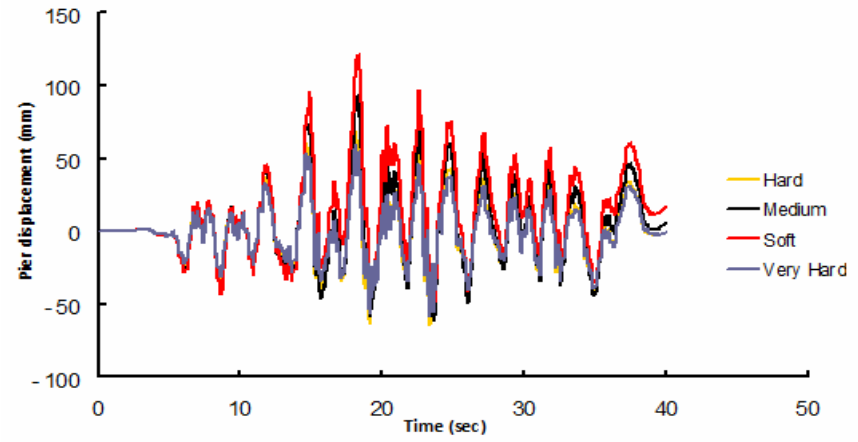

(a)

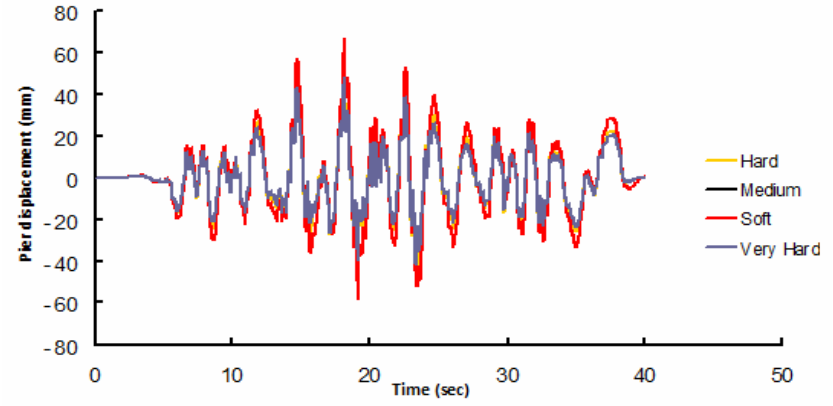

(b)

Fig. 4. Time-histories of the pier displacements subjected to (a) EQ-1 and (b) EQ-2 earthquake ground motion records. The legends show different ground conditions: very hard, hard, medium and soft soil conditions.

4.2 Bearing displacement

The bearing displacements are obtained from relative displacements between deck and pier. Figs. 6(a) and (b) present the time histories of shear strain of the isolation bearing (LRB) for the two earthquakes showing a very little difference in responses due to ground conditions in each earthquake. Figs. 7(a) and (b) present the shear stress-strain response of the LRB, obtained by using the Eqs. 2(a) to (d). Bearing displacements directly related to its energy dissipation capacity when subjected to seismic excitations. Bearing displacement increases with the decrease of energy dissipation of the bearings as revealed from Figs. 6(a) and (b). The peak shear strains of the LRB are presented in Figs. 8(a) and (b) illustrating that the isolation bearing experiences the least shear strain in soft soil condition for each earthquake, EQ-1 and EQ-2. However, the difference in shear strains of the LRB between the soft and very hard soils is not significant as revealed from Figs. 8(a) and (b). The numerical results as obtained for the isolation bearing in different ground conditions for the given earthquakes suggest that the effect of soil-structure interaction between foundation and surrounding soils can be suitably neglected. As per the damage states of the bearings defined in Table 7, the

peak shear strain of the isolation bearing (LRB), shown in Fig. 8(a), present moderate to extensive damages for EQ- 1 and slight to moderate damages for EQ-2, in all the ground condition, which has suggested that the ground condition has not significant effect on the seismic responses of LRB. The bearing displacement as obtained assuming a fully restrained condition at the base of the bridge pier is also superimposed in Figs. 8 (a) and (b).

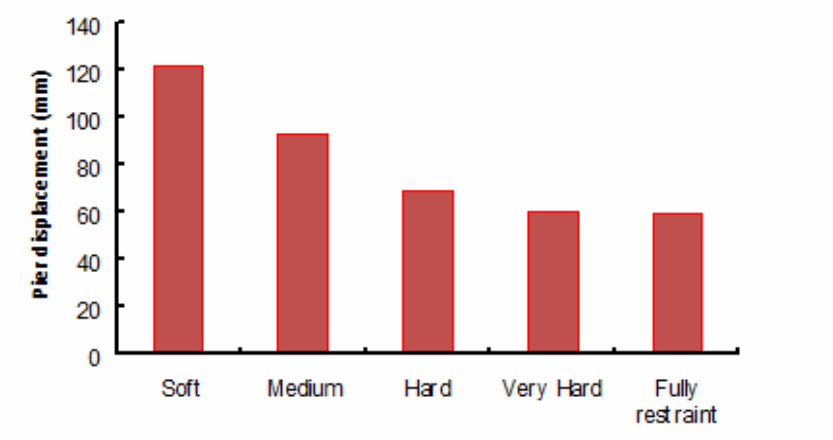

(a)

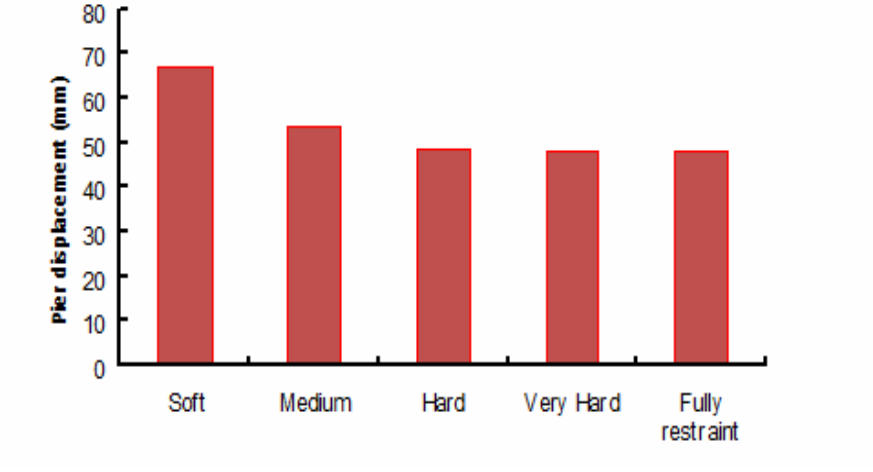

(b)

Fig. 5. Comparison of the peak responses of the pier displacement subjected to (a) EQ-1 and (b) EQ-2 earthquake ground motion records, for different ground conditions.

4.3 Deck displacement

Figs. 9(a) and (b) present the peak values of deck displacements of the bridge pier when subjected to earthquake ground motion records, EQ-1 and EQ-2. Looking at the results shown in Figs.9 (a) and (b), the deck displacements produced in soft ground condition appeared to be the highest of all ground conditions, for each earthquake. However, the difference of the deck displacements between the soft and very soils is not considerable. The direct reflection of these results can also be observed in the case of the bearing displacements. The deck displacement as obtained assuming a fully restrained condition at the base of the bridge pier is also superimposed in Figs. 9 (a) and (b).

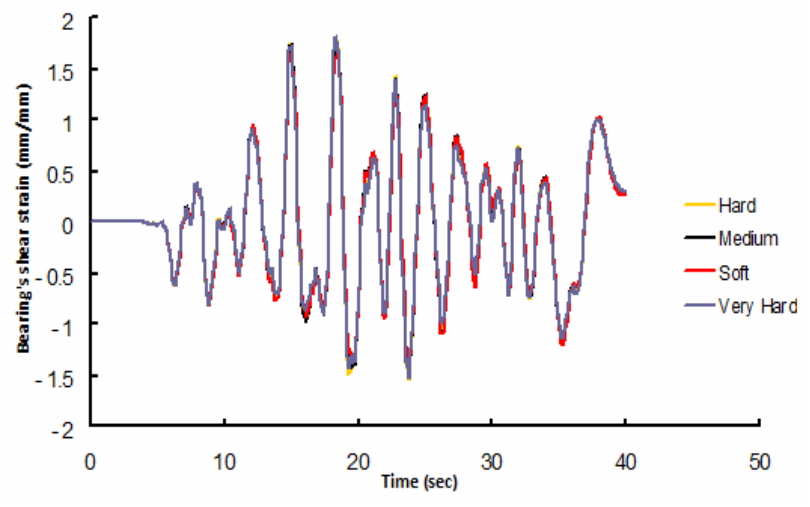

(a)

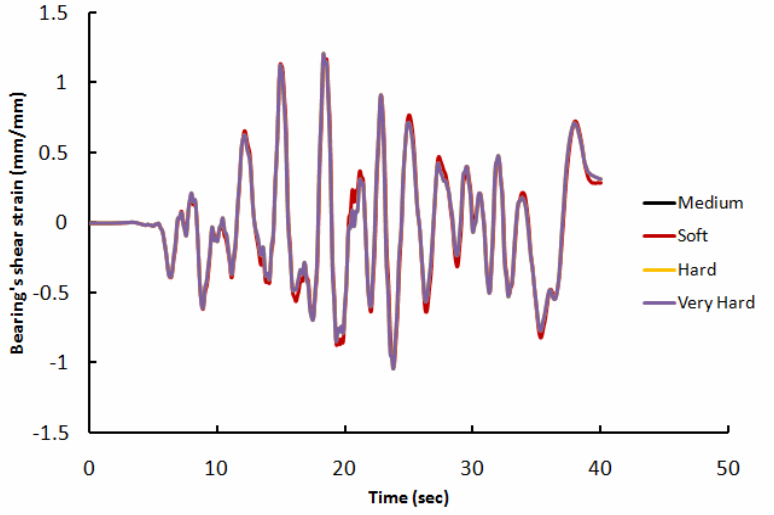

(b)

Fig.6. Time-histories of shear-strain of the isolation bearing of the bridge pier subjected to (a) EQ-1 and (b) EQ-2 earthquake ground motion records. The legends show different ground conditions: very hard, hard, medium and soft soil conditions.

4.3 Foundation movement

The peak displacements of the foundation of the bridge pier are presented in Figs. 10 (a) and (b), for different support/ground conditions, due to two earthquakes, EQ-1 and EQ-2. The numerical results shown in Figs.10 (a) and (b) show that the foundation displacements produced in soft ground condition appeared to be the highest of all ground conditions, for each earthquake. The foundation displacement as obtained assuming a fully restrained condition at the base of the bridge pier is also superimposed in Fig. 10. The direct reflection of these results can also be observed in the case of the pier displacements.

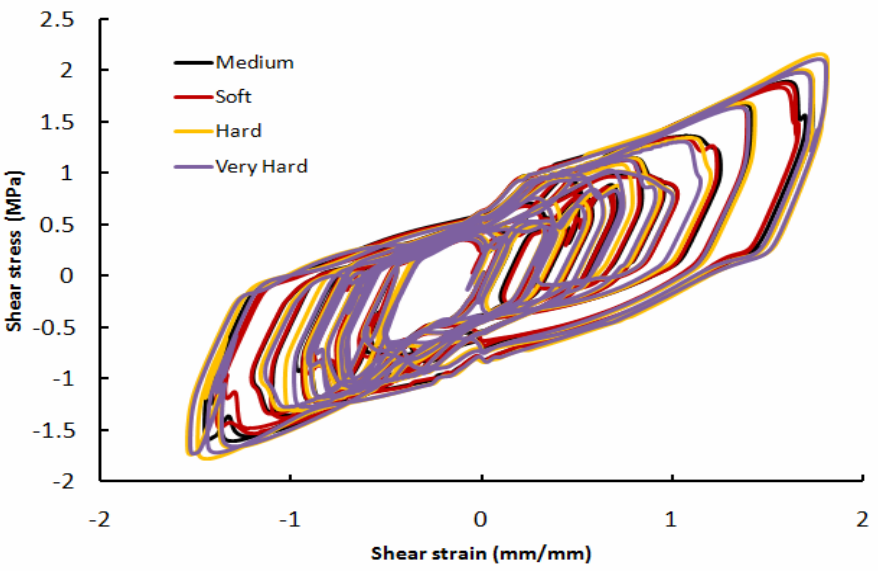

(a)

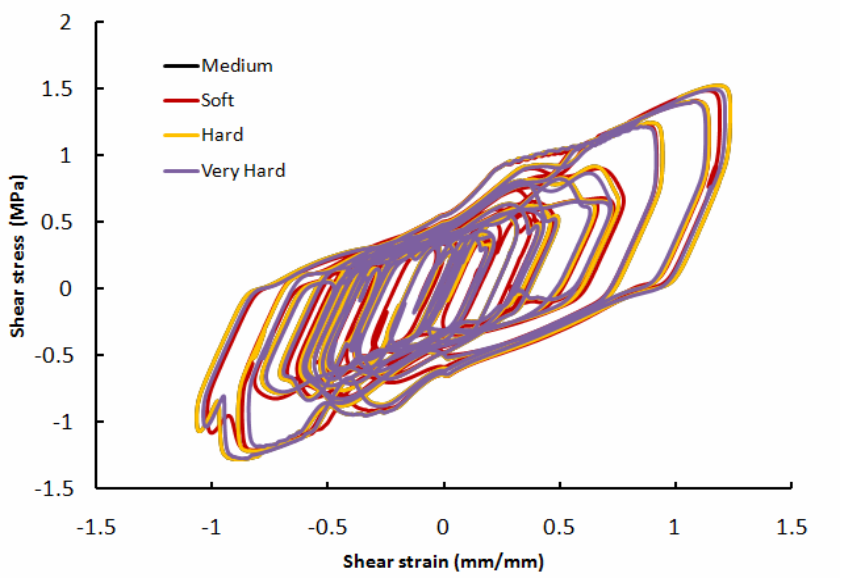

(b)

Fig.7. Shear force-shear strain behaviour of the isolation bearing of the bridge pier subjected to (a) EQ-1 and (b) EQ-2 earthquake ground motion records. The legends show different ground conditions: very hard, hard, medium and soft soil conditions

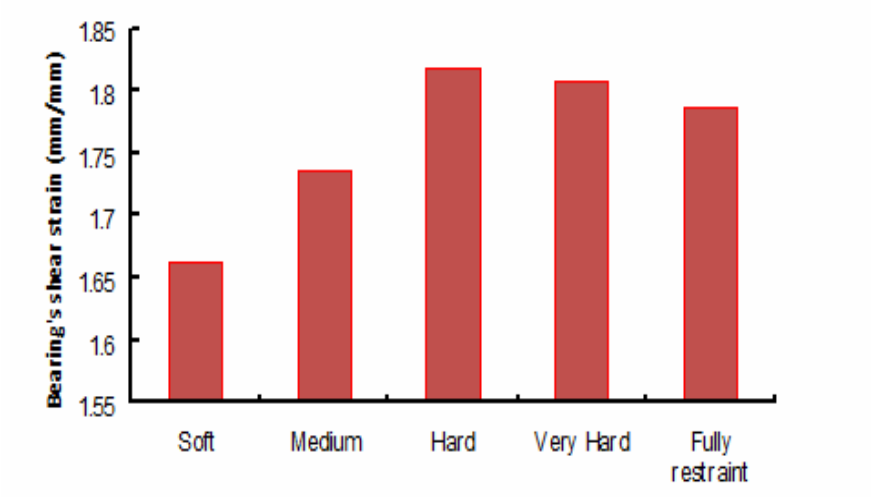

(a)

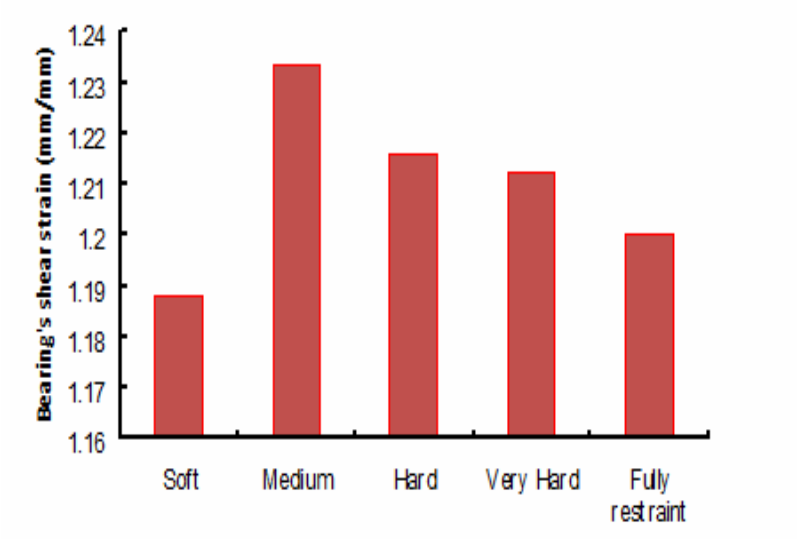

(b)

Fig. 8. Comparison of the peak responses of the bearing's shear-strain of the bridge pier subjected to (a) EQ-1 and (b) EQ-2 earthquake ground motion records, for different ground conditions.

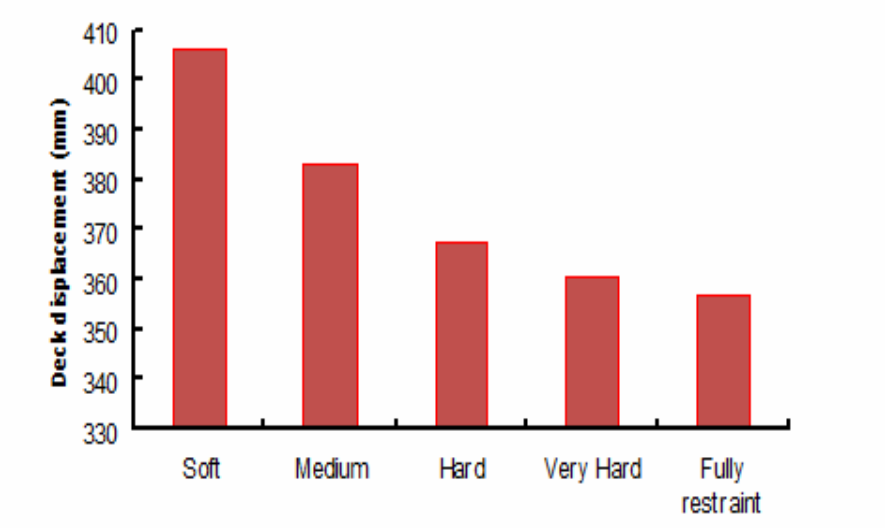

(a)

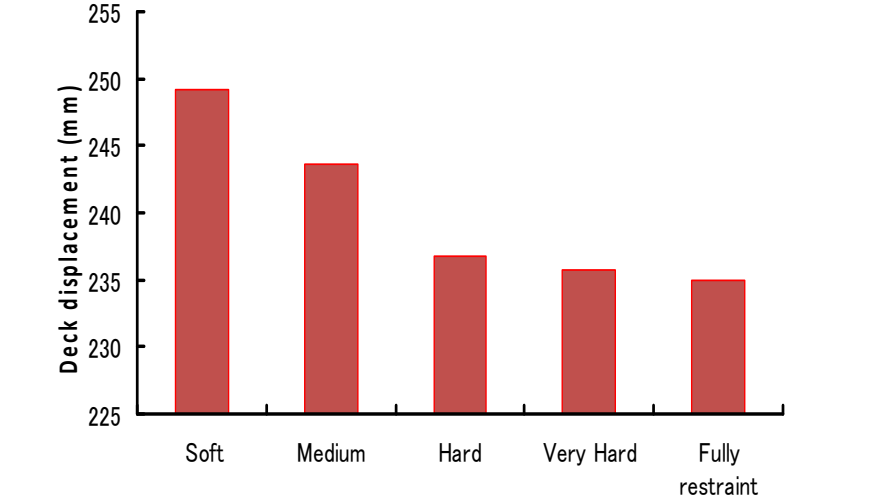

(b)

Fig.9. Comparison of the peak responses of the bridge deck bridge subjected to (a) EQ-1 and (b) EQ-2 earthquake ground motion records, for different ground conditions.

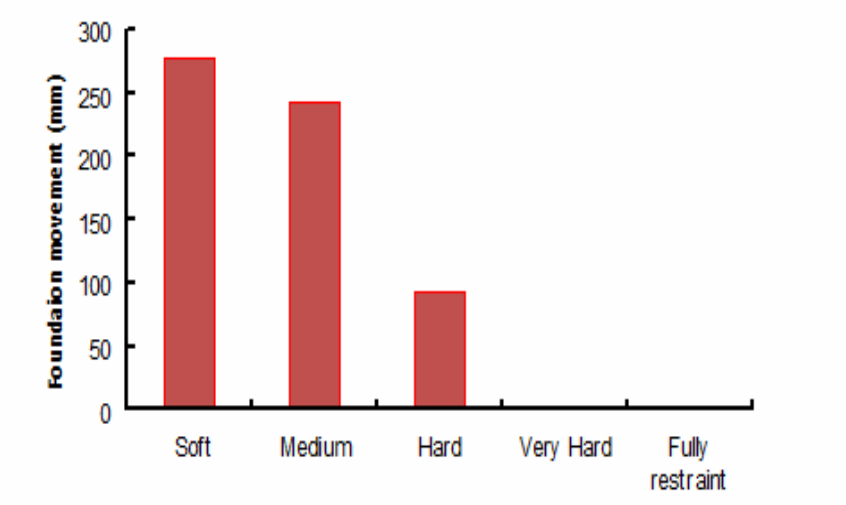

(a)

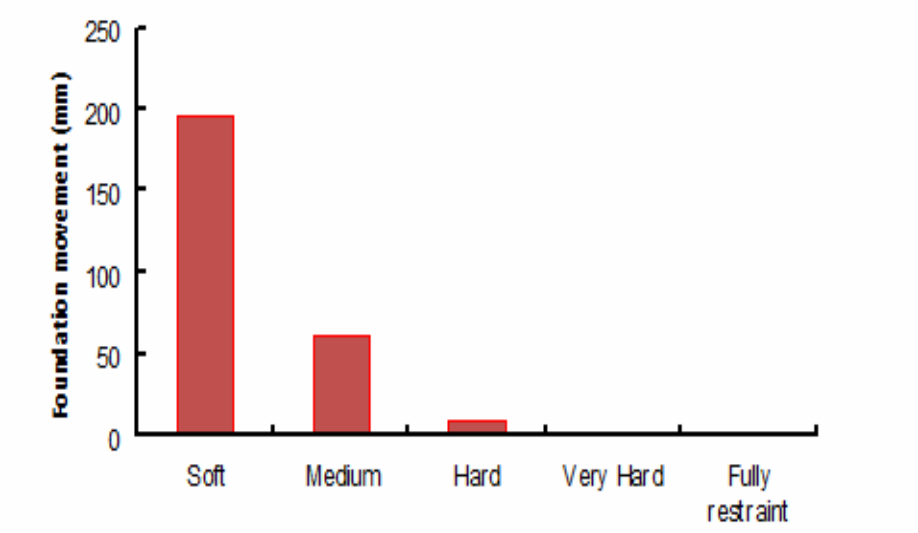

(b)

Fig.10. Comparison of the peak responses of the foundation movement due to (a) EQ-1 and (b) EQ-2 earthquake ground motion records, for different ground conditions.

5. Concluding remarks

This study presents the seismic performance assessment of a bridge pier modelled by 3-DOF system and isolated by laminated rubber bearing (LRB). The bridge is analysed for two earthquake ground acceleration records, namely EQ-1 and EQ-2. The nonlinearity of the bridge pier is considered by employing a bilinear force-displacement relationship, whereas a visco-elasto-plastic rheology model is employed to evaluate the mechanical behaviour of LRB under seismic excitations. The foundation-soil interaction has been introduced by an equivalent linear model.

The numerical results have revealed that the seismic responses of the bridge pier are significantly affected by the ground conditions representing the support conditions. For example, the pier displacement in soft ground condition is two times higher than that in very hard ground condition, when subjected to EQ-1. However, the difference in pier displacements between the soft and very hard soils becomes very small (i.e. about 25%) for

EQ-2. The consequence effect of this phenomenon has been reflected in the foundation movement of the bridge pier for each earthquake. It is also noted the bearing and deck displacements of the bridge pier are significantly affected by the ground conditions under the given earthquake ground motion records. From the numerical analysis conducted in the current study it can be revealed that the ground conditions at the base of the bridge pier (i.e support conditions) have significant effect on the seismic responses of the bridge, which should be carefully considered in the design phase of bridge system, particularly when seismic isolation bearings have been used.

In the current study, only one bridge pier under low to medium strong earthquake ground records is considered; however, a more rigorous modeling of the bridge system is expected for an elaborate numerical investigation since the seismic responses of such a simplified sub-assemblage would be different if the total assembly of the bridge is considered under different earthquake ground motion records considering duration, frequency contents and fault-line characteristics, etc. This is likely to change the dynamics of the entire bridge structure. This can be dealt with in a future work.

References

Bhuiyan, A. R. (2009), "Rheology modeling of laminated rubber bearings", PhD dissertation. Graduate School of Science and Engineering, Saitama University, Japan

Bhuiyan, A. R., Okui. Y., Mitamura, H., Imai, T. (2009), "A Rheology model of high damping rubber bearings for seismic analysis: identification of nonlinear viscosity", Int. Journal of Solids and Structures, 46, 1778-1792

Bhuiyan, A. R., Okui, Y. (2012), "Mechanical Characterization of Laminated Rubber Bearings and Their Modelling Approach" Earthquake Engineering, Chapter-12, InTech Publications, Europe

Chaudhary, M. T. A., Abe, M., and Fujino, Y. (2001), "Performance evaluation of base- isolated Yama-agé bridge with high damping rubber bearings using recorded seismic data", Engineering Structures 23, 902-910.

Dasgupta, S., Dutta, S. C and Bhattacharya, G. (1999) "Effect of soil-structure interaction on building frames on isolated footings" Journal of Structural Engineering (Madras), 26 (2), 129-134

Datta, T. K., (2010) "Soil-structure interaction" Seismic analysis of structures, Chapter-7, John Willey & Sons (Asia) Pte Ltd.

FEMA 450 (2003) "NEHRP recommended provisions for seismic regulations for new buildings and other structures" Building Seismic Safety Council (BSSC), Washington DC.

Ghobarah, A. (1988) "Seismic behavior of highway bridges with base isolation", Canadian Journal of Civil Engineering, 15, 72-78

Ghobarah, A., Ali, H. M. (1988) "Seismic performance of highway bridges", Engineering Structures, 10, 157-166

Hwang, J. S., Wu, J. D., Pan. T., Yang, G. (2002), "A mathematical hysteretic model for elastomeric isolation bearings", Earthquake Engineering and Structural Dynamics, 31, 771-789

Imai, T., Bhuiyan, A. R., Razzaq, M. K. Okui, Y. and Mitamura, H. (2010), "Experimental studies of rate-dependent mechanical behaviour of laminated rubber bearings", Joint Conference Proceedings, 7th International Conference on Urban Earthquake Engineering (7CUEE) & 5th International Conference on Earthquake Engineering (5ICEE), March 3-5, 2010, Tokyo Institute of Technology, Tokyo, Japan

Japan Road Association (JRA) (1996), "Specifications for highway bridges-Part V: Seismic design", Tokyo, Japan.

Japan Road Association (JRA) (2002), "Specifications for highway bridges-Part V: Seismic design", Tokyo, Japan.

Kelly, J. M. (1997), "Earthquake resistant design with rubber", 2nd edition, Springer-Verlag Berlin Heidelberg, New York

Kikuchi, M., Aiken, I. D. (1997), "An analytical hysteresis model for elastomeric seismic isolation bearings" Earthquake Engineering and Structural Dynamics, 26, 215-231.

Miehe, C. and Keck, J. (2000), "Superimposed finite elastic-viscoplastic-plasto-elastic stress response with damage in filled rubbery polymers:Experiments, modeling and algorithmic implementation", Journal of Mechanics and Physics of Solids, 48,323-365.

Naeim, F., and Kelly, J. (1996), "Design of seismic isolated structures", 1st edition, John Wiley and Sons, New York

Ozbulut, O. E., Hurlebaus, S. (2011a), "Optimal design of superelastic-friction base isolators for seismic protection of highway bridges against near-field earthquakes", Earthquake Engineering and Structural Dynamics, 40, 273–291

Ozbulut, O. E., Hurlebaus, S. (2011b), "Seismic assessment of bridge structures isolated by a shape memory alloy/rubber-based isolation system", Smart Materials and Structures, 20

Priestley, M. J. N., Seible, F. and Calvi, G. M., 1996. "Seismic design and retrofit of bridges", John Wiley and Sons, New York

Razzaq, M. K., Bhuiyan, A.R., Okui, Y., Mitamura, H. and Imai, T. (2010), " Effect of rubber bearings modelling on seismic response of base", Joint Conference Proceedings, 7th International Conference on Urban Earthquake Engineering (7CUEE) & 5th International Conference on Earthquake Engineering (5ICEE), March 3-5, 2010, Tokyo Institute of Technology, Tokyo, Japan

Resp-T (2006). "User's Manual for Windows, Version 5"

Saiidi, M., 1982. "Hysteresis models for reinforced concrete", Journal of Structural Engineering, 108, 1077-1087

Skinner, R.I., Robinson, W. H., McVerry, G.H. (1993), "An introduction to seismic isolation", DSIR Physical Science, Wellington, New Zealand

Takeda, T., Sozen, M.A., and Nielsen, N.N., (1970)"Reinforced concrete response to simulated earthquakes", Journal of Structural Engineering, 96, 2557-2573

Todorovska, M. I., (1996), "Soil-structure interaction for base-isolated buildings", Proceedings of 11th Conference on Engineering Mechanics, ASCE, Volume 1, 172-175

Tongaonkar NP, Jangid RS. "Seismic response of isolated bridges with soil–structure interaction", Soil Dynamics and Earthquake Engineering 2003; 23(4):287–302

Vlassis, A. G. and Spyrakos, C.C. (2001), "Seismically isolated bridge piers on shallow soil stratum with soil-structure interaction", Computers and Structures, 79 (32), 2847-2861.1

Wilde. K., Gardoni, P., Fujino, Y. (2000), "Base isolation system with shape memory alloy device for elevated highway bridges", Engineering structures, 22, 222–229.

Zhang, J., Huo, Y. (2009), "Evaluating effectiveness and optimum design of isolation devices for highway bridges using the fragility function method", Engineering Structures, 31, 1648-1660;